

NASA-CR-172,442

# NASA Contractor Report 172442

NASA-CR-172442  
19840025525

A THEORETICAL STUDY OF RESIN FLOWS FOR THERMOSETTING  
MATERIALS DURING PREPREG PROCESSING

## FOR REFERENCE

NOT TO BE TAKEN FROM THIS ROOM

T. H. Hou

Kentron International, Inc.  
Aerospace Technologies Division  
Hampton, Virginia 23666

Contract NAS1-16000  
July 1984

**LIBRARY COPY**

OCT 16 1984

LANGLEY RESEARCH CENTER  
LIBRARY, NASA  
HAMPTON, VIRGINIA

**NASA**

National Aeronautics and  
Space Administration

Langley Research Center  
Hampton, Virginia 23665



DISPLAY 05/2/1

84N33596\*# ISSUE 23 PAGE 3724 CATEGORY 27 RPT#: NASA-CR-172442 NAS  
1.26:172442 CNT#: NAS1-16000 84/07/00 34 PAGES UNCLASSIFIED  
DOCUMENT

UTTL: A theoretical study of resin flows for thermosetting materials during  
prepreg processing TLSP: Final Report

AUTH: A/HOU, T. H.

CORP: Kentron International, Inc., Hampton, Va. AVAIL. NTIS SAP: HC A03/MF  
A01

MAJS: /\*COMPRESSIBLE FLOW/\*FLOW THEORY/\*FLOW VISUALIZATION/\*POROUS MATERIALS/\*  
PREPREGS/\*THERMOSETTING RESINS

MINS: / MATHEMATICAL MODELS/ PLASTIC PROPERTIES/ THERMOPLASTIC RESINS

ABA: E. A. K.

ABS: A flow model which describes the process of resin consolidation during  
prepreg lamination was developed. The salient features of model  
predictions were explored. It is assumed that resin flows in all  
directions originate from squeezing action between two approaching  
adjacent fiber/fabric layers. In the horizontal direction, a squeezing  
flow between two nonporous parallel plates is analyzed, while in the  
vertical direction a Poiseuille type pressure flow through porous media is  
assumed. Proper force and mass balance was established for the whole  
system which is composed of these two types of flow. A flow parameter, CF,  
shows to be a measure of processability for the curing resin. For a given

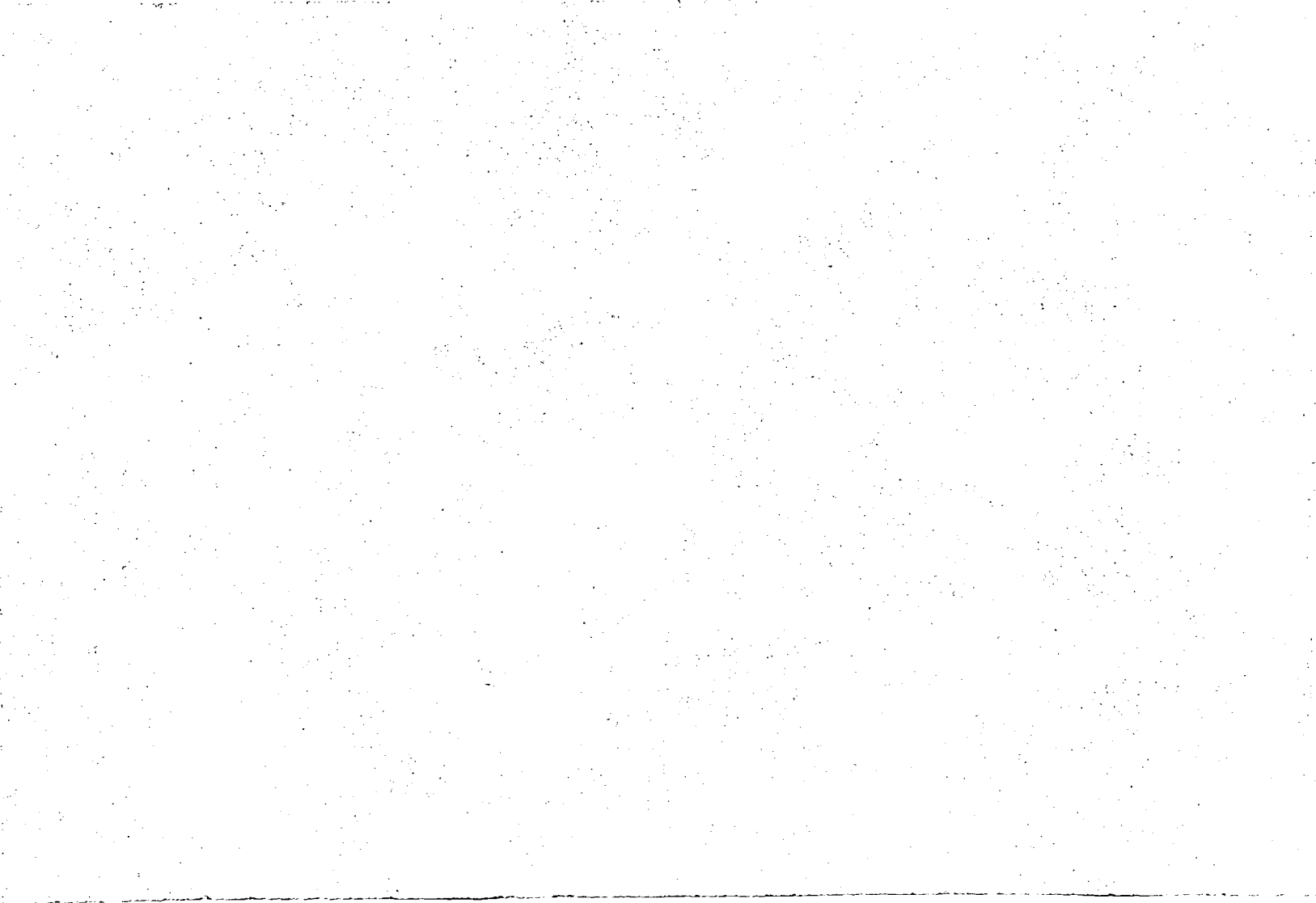


## TABLE OF CONTENTS

	<u>Page</u>
List of Figures	ii
Foreword	iii
Abstract	iv
List of Symbols	v
I. Introduction	1
II. Theory	3
Physical Model	3
Mathematical Formulation	3
A. Vertical Flow Through Porous Media	3
B. Horizontal Squeezing Flow	4
III. Numerical Results and Discussions	8
IV. Conclusions	13
References	14

## LIST OF FIGURES

<u>Figure</u>	<u>Title</u>	<u>Page</u>
1.	Schematic diagram of multilayer prepreg laminate	
2.	Resin flow - physical model	
3.	Compression data for 1080 glass fabric (Bartlett, Ref. 2)	
4.	Changes of prepreg thickness vs. flow parameter at different values of applied load, $F$	
5.	Changes of prepreg thickness vs. flow parameter at different values of $C_Z Z_0$	
6.	Chemoviscosity of a hypothetical B-stage epoxy resin at 150°C (423°K)	
7.	Variations of prepreg thickness as a function of time for different values of $C_Z Z_0$	
8.	Rate of change of prepreg thickness as a function of time for different values of $C_Z Z_0$	
9.	Changes of prepreg thickness vs. flow parameter at different values of $C_Z Z_0$	
10.	Changes of prepreg thickness vs. applied load at different values of flow parameter $C_F$	
11.	Changes of prepreg thickness vs. external load at different values of $C_Z Z_0$	
12.	Volumetric resin flow in the vertical direction as a function of time at different values of $C_Z Z_0$	

## FOREWORD

This work, performed at the NASA Langley Research Center, represents progress on an ongoing research effort for the development of an analytical model for thermoset prepregging processes in autoclave fabrication applications. The work was supported under NASA Contract NAS1-16000. Mr. R. M. Baucom (PMB) is Technical Monitor for this project. This work was performed by Dr. T. H. Hou of Kentron International, Inc.

## ABSTRACT

A new flow model which describes the process of resin consolidation during prepreg lamination has been developed. A parametric study has also been carried out to explore the salient features of model predictions. It is assumed that resin flows in all directions are originated from squeezing action between two approaching adjacent fiber/fabric layers. In the horizontal direction, a squeezing flow between two nonporous parallel plates is analyzed, while in the vertical direction a poiseuille type pressure flow through porous media is assumed. Proper force and mass balances have been established and solved for the whole system which is composed of these two types of flow.

A flow parameter,  $C_F$ , has been defined and shown to be a measure of processability for the curing resin. For a given external load  $F$  the responses of resin flow during prepreg lamination, as measured by  $C_F$ , are categorized into three regions: the low  $C_F$  region where resin flows are inhibited by the high chemoviscosity during initial curing stages; the median  $C_F$  region where resin flows are properly controllable; and the high  $C_F$  region where resin flows cease due to fiber/fabric compression effects. Resin losses in both directions can be calculated as well.

Potential uses of this model, including quality control of incoming prepreg material, are discussed. Experimental measurements needed to confirm the prepreg characterization methods suggested by the model have been planned for future research. The parallel-plate plastometer will be an appropriate device to carry out the experiments.



## LIST OF SYMBOLS

$A_z$	Area ( $\text{cm}^2$ ) perpendicular to the z-direction
$C_F$	Flow Parameter ( $\text{cm}^2/\text{dyne}$ ) defined in Eq. (11)
$C_z$	$\equiv dp/dz$ (psi/cm)
$\Delta E_n$	Viscous flow Activation Energy (Kcal/mole)
$\Delta E_k$	Viscosity cure Activation Energy (Kcal/mole)
$F$	External loading (dynes)
$h(t)$	Separation (cm) between parallel plates
$h_0$	Initial separation (cm) between parallel plates
$1 - h(t)/h_0$	A measure of plate separation (Fig. 2) at any instant $t$ as a fraction of the original distance $h_0$
$\dot{h}(t)$	$\equiv dh/dt$ (cm/sec)
$K$	Permeability ( $\text{cm}^2$ ) of porous material
$k$	Viscosity rate constant
$k_\alpha$	Material constant ( $\text{min}^{-1}$ )
$p$	Pressure (psi) generated by squeezing action between two approaching plates
$p_a$	Ambient pressure (psi)
$p_G$	Pressure (psi) absorbed by glass fabric or fiber bundles
$Q_1, Q_2$	Defined by Eq. (10)
$Q_r, Q_z$	Volumetric resin flow ( $\text{cm}^3$ ) in $r$ and $z$ direction, respectively
$Q_T$	Total volumetric resin flow ( $\text{cm}^3$ )
$R$	Universal gas constant (Kcal/mole $^\circ\text{K}$ )
$r, \theta, z$	Cylindrical coordinate system
$T$	Curing temperature ( $^\circ\text{K}$ )

$t$	Curing time (sec)
$V_0$	Velocity (cm/sec) averaged over a small region of space in porous material
$V_r, V_z$	Velocity (cm/sec) in $r$ and $z$ direction, respectively
$Z_0$	Characteristic thickness (cm) of porous material where resin flows
$\eta(t)$	Chemoviscosity (poise)
$\eta_0$	Initial viscosity (poise) at $t = 0$
$\eta_\infty$	Material constant (poise)
$\rho$	Density (gm/cm <sup>3</sup> ) averaged over a region in porous material

## I. INTRODUCTION

High quality fiber reinforced composites, such as those used in aerospace and industrial applications, are commonly processed in autoclaves. During processing, the composite materials are subjected to prescribed elevated temperatures and pressures. Selection of a cure cycle (temperature profile) will dictate the kinetics of polymer chemical reactions and the viscosity growth profile. In order to maintain control over these parameters an adequate chemoviscosity model is required. During processing, increased molding pressure results in resin flow both perpendicular and parallel to the fibers. The applied pressure helps to consolidate the composite laminates and to squeeze out excess resin. An adequate resin flow model for the entire system (laminate/bleeder/breather) is needed to provide a description of the time-dependent laminate consolidation process by analyzing the flow pattern, loss of resin, and pressure profiles during processing.

Considerable work has been conducted in the past by numerous researchers in searching for a relationship between chemoviscosity and cure kinetics.<sup>1</sup> However, the mechanics governing the flow of resin associated with composite laminate processing has received little attention. Bartlett<sup>2</sup> developed a theoretical flow model for glass-reinforced resin during lamination for multilayer printed circuit boards in the electronics industry. His model assumed that the glass fabric behaves as a porous media; that the flow over and through the glass bundles offers the greatest resistance to flow (i.e., resin flow in perpendicular direction is negligible); and that the lamination process is isothermal. A poiseuille type of flow was assumed for the horizontal directions. The unique features of Bartlett's model are that (i) the specific permeability of the porous glass reinforcement is considered a function of fabric geometry; and (ii) the effect of layers of glass fabric coming into contact with one another as the resin is squeezed out has been taken into account. The model was later compared with experimental results by Bloechle<sup>3,4</sup> using a parallelplate plastometer, and was successfully applied to quality control of incoming epoxy B-stage prepregs in a manufacturing environment.

Springer and Loos<sup>5-8</sup> considered resin flows perpendicular and parallel to the planes of the composite. Darcy's law for flow through porous materials was assumed in the vertical direction, while poiseuille type pressure flow was

analyzed in the parallel direction. Macroscopic force and mass balances were performed in each direction from which the approaching speeds  $dh/dt$  for two adjacent layers of porous plates separated by a distance of  $2h$  (see fig. 2), and the amount of resin loss was derived. Experiments were conducted with Hercules AS/3501-6 graphite epoxy prepreg and the model predictions were shown to compare favorably with the experimental data for multiple laminates.

Lindt<sup>9</sup> studied the flow mechanics associated with the formation of fiber reinforced composite laminates. The overall flow pattern in the laminate was conceptually compartmentalized into units of a flow cell. Each individual cell is composed of two types of flow - a squeezing flow in the horizontal direction between two fiber layers, and a poiseuille type pressure flow in the vertical direction. Both are originated from the squeezing action between two adjacent fiber layers. Lubrication approximation is employed to formulate the equations of equilibrium. Numerical solutions reveal reasonable patterns of fiber distribution, loss of resin, flow field, and pressure profiles in the laminate. No experimental comparisons have been reported, however.

In this report, a newly developed resin flow model for composite processing will be described. It is assumed that flows in both vertical and horizontal directions originate from the squeezing action between adjacent fiber layers. A parametric study has been performed to illustrate the salient features of the model predictions with regard to the relationships between process conditions and material responses. Only the case of isothermal cure has been considered in this study.

## II. THEORY

### Physical Model

The schematic diagram of a composite laminate is shown in Fig. 1. A stack of 5 layers of prepreg tapes is confined between two steel plates and layers of porous materials. The porous materials include those commonly called bleeder and breather materials. When a force,  $F$ , is applied, the resin flow pattern observed by Springer<sup>7</sup> indicates that the first (top) layer moves toward the second one, while the resin is squeezed out from the space between the two layers. Simultaneously, a similar situation holds for the bottom layer. When the first layer reaches the second one, the two layers will move together toward the third layer, squeezing resin out of the space between the second and third layers. This sequence is repeated for the subsequent layers. One important observation noted by Springer is that upon application of the force  $F$ , the first (top) plate moves downward (or upward for the bottom plate in Fig. 1). A plate further down starts moving only when the plates above reach it.

A typical flow channel between two layers of prepreg tapes is shown schematically in Fig. 2(a). Resin is confined between parallel porous plates separated by a distance,  $h$ . Upon application of a force,  $F$ , the resin is squeezed outward horizontally and also vertically through the porous media. It is assumed that these two flow directions can be decoupled conceptually as shown in Fig. 2(b) and (c). Fig. 2(b) illustrates a squeezing flow between two non-porous plates separated by a same distance,  $h$ , as in Fig. 2(a). A vertical pressure flow through porous materials is illustrated in Fig. 2(c) (assuming no horizontal flow), and that flow through the porous materials is driven by a pressure drop ( $p - p_a$ ) across a characteristic distance,  $Z_0$ , where  $p$  is the pressure generated by the squeezing action between plates, and  $p_a$  is the ambient pressure. The same external force,  $F$ , is applied in Fig. 2(b) and (c).

### Mathematical Formulation

#### A. Vertical Flow Through Porous Media

For the flow of a fluid through a porous medium, the equation of motion can be replaced by Darcy's law<sup>10</sup>

$$\underline{V}_0 = - \frac{K}{\eta} (\nabla p - \rho \underline{g}), \quad (1)$$

where the underlined quantities denote vectors.  $K$  is the permeability of the porous medium,  $\eta$  is the viscosity,  $\underline{V}_0$  is a superficial velocity averaged over a small region of space, and  $\rho$  and  $p$  are density and pressure, respectively, averaged over a region available to flow that is large with respect to the pore size.

For an incompressible liquid and constant  $K$  and  $\eta$ , Eq. (1) together with the equation of continuity can be reduced to

$$\nabla^2 p = 0 \quad (2)$$

As a first order approximation, we assume that Eq. (2) is applicable to our system (Fig. 2(c)) in a unidirectional flow. Eqs. (1) and (2) can then be combined to give

$$V_0 = \frac{K}{\eta} C_z, \quad (3)$$

where  $C_z = dp/dz$  is a constant. The volumetric resin flow in the (vertical)  $z$ -direction is therefore equal to

$$Q_z = A_z C_z K \int_0^t \frac{1}{\eta(t)} dt \quad (4)$$

where  $A_z$  is area perpendicular to the  $z$ -direction and  $\eta(t)$  is the chemoviscosity of the reacting resin.

#### B. Horizontal Squeezing Flow

We now consider the squeezing flow between two non-porous plates, as shown in Fig. 2(b). A cylindrical coordinate system  $(r, \theta, z)$  is chosen for convenience. The velocity and pressure fields are assumed  $V_r = V_r(r, z)$ ,  $V_z = V_z(z)$  and  $p = p(r)$  only. The equation of continuity becomes

$$2\pi r \int_0^h v_r dz + \pi r^2 (\dot{h} + v_0) = 0, \quad (5)$$

where  $\dot{h} = dh/dt$  is a measure of the speed of two approaching parallel plates upon the application of force  $F$ , and  $v_z = \dot{h}$  at  $z = h$ .

For the velocity field assumed, Bird et al.<sup>11</sup> have shown that the  $r$ -component equation of motion can be integrated to give

$$v_r = \frac{h^2 r}{2} \left( -\frac{1}{\eta r} \frac{dp}{dr} \right) \left[ 1 - \left( \frac{z}{h} \right)^2 \right] \quad (6)$$

Substituting Eq. (6) into Eq. (5), we have

$$\frac{dp}{dr} = \frac{3}{2} \frac{\eta r}{h^3} (\dot{h} + v_0), \quad (7)$$

which can then be integrated to obtain the pressure distribution as

$$p(r) - p_a = -\frac{3}{4} \eta \frac{R^2}{h^3} (\dot{h} + v_0) \left[ 1 - \left( \frac{r}{R} \right)^2 \right] \quad (8)$$

Eq. (8) represents the squeezing generated pressure drop between two parallel plates approaching with a speed  $\dot{h}(t)$ . By equating a balance in force, we have

$$F = \int_0^R \left[ (p(r) - p_a) + C_z Z_0 + P_G \right] 2\pi r dr \quad (9)$$

$$= \pi R^2 (C_z Z_0 + P_G) - \frac{3}{8} \pi \frac{R^4}{h^3} [\eta \dot{h} + K C_z],$$

where  $F$  is the applied external force to the plates, and  $P_G$  is the pressure absorbed by the glass fabric or fiber bundles. Physically it is noted that when

layers of fibers come into contact with one another as the resin is squeezed outward, they begin to carry a portion of the applied load. The average pressure applied to the resin is therefore the difference between the average applied pressure and the pressure  $P_G$  carried by the fibers.  $P_G$  was shown to be a function of distance  $h$  by Bartlett<sup>2</sup>. Eq. (9) can be rearranged to become:

$$\int_0^t \frac{1}{\eta(t)} dt = - \int_{h_0}^h \frac{1}{KC_z + \left(\frac{F - Q_1}{Q_2}\right)h^3} dh, \quad (10)$$

with

$$Q_1 = \pi R^2 (C_z Z_0 + P_G),$$

and

$$Q_2 = \frac{3}{8} \pi R^4$$

For a given fabric subjected to a known load  $F$ , Eq. (10) then relates the plates approaching characteristics  $h(t)$  to the change of chemoviscosity (rate of cure) of thermosetting resin. A quantity called the flow parameter,  $C_F$ , can therefore be defined as:

$$C_F = \int_0^t \frac{1}{\eta(t)} dt. \quad (11)$$

The significance of  $C_F$  will be discussed in the following section.

Substituting Eq. (7) into Eq. (6), we have

$$v_r(r, z) = -\frac{3}{4} \frac{r}{h} (\dot{h} + v_0) \left[1 - \left(\frac{z}{h}\right)^2\right], \quad (12)$$



and  $Q_r$ , the volumetric edge resin loss, can be calculated. A more direct method is to calculate the total resin loss,  $Q_T$ , as

$$Q_T = - A_z \int_0^t \dot{h} dt, \quad (13)$$

and then  $Q_r$  can be obtained from

$$Q_r = Q_T - Q_z, \quad (14)$$

where  $Q_z$  is calculated by Eq. (4).

### III. Numerical Results and Discussions

For the purposes of illustrating unique features of model predictions discussed previously, a 1080 B-stage glass fabric material used by Bloechle<sup>3</sup> was chosen. Permeability,  $K$ , of the material is  $5.8 \times 10^{-12} \text{cm}^2$ . The load-deformation characteristics of the same material has been reported by Bartlett<sup>2</sup> and is also reproduced in Fig. 3.

From Eqs. (10) and (11), we have

$$C_F = \int_0^t \frac{1}{\eta(t)} dt = - \int_{h_0}^h \frac{1}{KC_z + \left(\frac{F - Q_1}{Q_2}\right)h^3} dh \quad (15)$$

For a pair of parallel plates with a radius  $R = 7.45 \text{ cm}$  separated initially by a distance  $h_0 = 9.144 \times 10^{-3} \text{ cm}$ , Eq. (16) can be solved for fixed value of pressure gradient,  $C_z$ , in vertical flow through a porous media as shown in Fig. 4, or for a fixed value of external load  $F$ , as shown in Fig. 5. The quantity  $1-h/h_0$  in the vertical axis represents a measure of processibility or resin flow, and is shown to be related directly to the flow parameter  $C_F$ . Similar characteristics are noted to exist for each curve in Fig. 4. In the region of low  $C_F$  where values of  $1-h/h_0$  are relatively unchanged, the flow characteristic is dominated by chemoviscosity changes in the resin during the initial curing stages (see Eq. (15)). In the middle region of each curve where values of  $1-h/h_0$  are most sensitive to  $C_F$ , resin flows can be properly controlled by adjusting the values  $F$ ; namely, more excess resin can be squeezed out for higher applied loads. As the values of  $C_F$  increase, a plateau region for each curve becomes apparent. In this plateau region, values of  $1-h/h_0$  become insensitive to changes in  $C_F$  again since adjacent fiber or fabric layers nest together and are compressed against each other. At this stage fibers carry the major portion of the load and the resins cease to flow.

It can be noted from Fig. 4 that reductions in the external applied load  $F$  shift the curves to the higher  $C_F$  region. The maximum attainable resin flow  $1-h/h_0$  is also reduced. Both of these behaviors are consistent with the above arguments. Upon application of two different loads with  $F^1 < F^2$ , the corresponding horizontal shift between two curves in Fig. 4 can be calculated by

$$C_F^1 - C_F^2 = \int_{t_1}^{t_2} \frac{1}{\eta(t)} dt = \int_{h_0}^h \frac{h^3(F_2-F_1)/Q_2}{[KC_Z + (\frac{F_1-Q_1}{Q_2})h^3] [KC_Z + (\frac{F_2-Q_1}{Q_2})h^3]} dh, \quad (16)$$

and is shown to be a function of distance,  $h$ .

Fig. 5 shows the effects of the magnitude of  $C_Z Z_0$ .  $C_Z Z_0$  is the pressure drop which drives the resin to flow vertically through the porous media. Increasing the magnitude of  $C_Z Z_0$  has a similar effect to decreasing the external load  $F$  as discussed in Fig. 4. The horizontal shift between two curves of different  $C_Z Z_0$  values can be calculated by

$$C_F^1 - C_F^2 = \int_{t_1}^{t_2} \frac{1}{\eta} dt \quad (17)$$

$$= \int_{h_0}^h \left[ \frac{1}{KC_Z^1 + (\frac{F-Q_1}{Q_2})h^3} - \frac{1}{KC_Z^2 + (\frac{F-Q_1}{Q_2})h^3} \right] dh,$$

for  $(C_Z Z_0)_1 > (C_Z Z_0)_2$ . The amount of shift  $(C_F^1 - C_F^2)$  due to changes in magnitude of  $C_Z Z_0$  is, however, smaller than that due to changes in the magnitude of external load  $F$ , as can be seen by comparing Figs. 4 and 5.

The B-stage epoxy viscosity can be represented by<sup>2</sup>

$$\eta(t) = \eta_0 \exp [kt], \quad (18)$$

with

$$\eta_0 = \eta_\infty \exp [\Delta E_\eta / RT],$$

and

$$k = k_\infty \exp [-\Delta E_k / RT],$$

where  $\eta$  and  $\eta_0$  are curing and initial viscosity, respectively;  $k$  is the viscosity rate constant;  $\Delta E_\eta$  and  $\Delta E_k$  are viscous flow and cure activation energy, respectively; and  $\eta_\infty$  and  $k_\infty$  are two material constants. The viscosity is plotted as a function of time in Fig. 6. A linear dependence of the viscosity with respect to the logarithm of curing time has been commonly observed for many thermosetting resins. Values of parameters defined in Eq. (15) are tabulated below.

Table I. Values of parameters defined in Eq. (18).

---

$\eta_\infty$	$= 3.78 \times 10^{-13}$ poises
$k_\infty$	$= 5.5 \times 10^9 \text{ min}^{-1}$
$\Delta E_\eta$	$= 28 \text{ Kcal/mole}$
$\Delta E_k$	$= 20 \text{ Kcal/mole}$
$R$	$= 1.982 \times 10^{-3} \text{ Kcal/mole } ^\circ\text{K}$
$T$	$= 423^\circ\text{K}$

---

By knowing resin chemoviscosity  $\eta(t)$  (Fig. 6) and fabric or fiber compression characteristics  $P_G(h)$  (Fig. 3), it is possible to calculate the laminate thickness  $h(t)$  under a constant loading  $F$  by Eq. (10). The rate of decrease of the laminate thickness  $h(t)$  can be calculated by rearranging Eq. (9) so that

$$\frac{dh}{dt} = - \frac{1}{\eta(t)} \left[ KC_z + \frac{F-Q_1}{Q_2} h^3 \right], \quad (19)$$

where  $Q_1$  and  $Q_2$  are previously defined by Eq. (10).

Calculated values of  $h(t)$  are plotted in Fig. 7 for different values of  $C_Z Z_0$ . As expected, the larger magnitudes of  $C_Z Z_0$  result in thicker laminates. The rate of decrease in laminate thickness,  $dh/dt$ , is plotted for different values of  $C_Z Z_0$  in Fig. 8. Similar to  $h(t)$ , larger magnitudes of  $C_Z Z_0$  are noted to result in lower values of  $dh/dt$ . Nearly linear relationships between  $\ln(dh/dt)$  and  $t$  are observed for the range of values of  $C_Z Z_0$  discussed herein.

Values of the flow parameter  $C_F$  are also calculated and plotted against  $1-h/h_0$  in Fig. 9 for different values of  $C_Z Z_0$ . By comparing Figs. 5 and 9 it can be seen that the present experiments have not reached the second plateau region (high  $C_F$  in Fig. 5) where fiber-fiber compression becomes dominant and the resin ceases to flow. It can be noted in Fig. 7 that the resin ceases to flow between 10 and 20 minutes after the load  $F = 1.39 \times 10^8$  dynes has been applied. This is due to the fast increase in chemoviscosity of the resin.

In Fig. 10,  $1-h/h_0$  is plotted against external load  $F$  for constant values of  $C_F$  according to Eq. (15). As  $F$  increases,  $1-h/h_0$  approaches its limiting value of 1.0. A higher value of the flow parameter  $C_F$  implies lower viscosity resin, and  $1-h/h_0$  approaches 1.0 at lower external loads, as expected. It should be emphasized that the quantity  $1 - h(t)/h_0$ , as defined in Fig. 2, is a measure of separation between two individual parallel prepreg layers at any instant during laminate processing, and is not a direct measurement of the change of thickness of the multi-layer laminate. The change of laminate thickness as a whole can, however, be calculated from  $(1 - h/h_0)$  by taking the fiber/fabric thicknesses into account. The curves shown in Fig. 10 are useful in establishing quality control of prepreg materials. For a given prepreg tape,  $C_F$  should be a constant if the load  $F$  is applied for a fixed period of time according to Eq. (11). The experiments to verify the curves in Fig. 10 are easy to implement in principle by means of a plastometer, and the validity of the assumption that  $C_Z Z_0$  is a constant (instead of a function of  $h$ ) throughout the tests can therefore be evaluated.

A similar plot of  $1-h/h_0$  versus  $F$  for different values of  $C_Z Z_0$  is shown in Fig. 11. Because higher values of  $C_Z Z_0$  result in lower values of  $dh/dt$  as discussed previously in regard to Fig. 8, the shifts of the curves to the higher  $F$  region on these plots as values of  $C_Z Z_0$  become larger are

expected. Figure 11 is constructed for a fixed value of  $C_F = 0.01$ , and is particularly useful as a complement to Fig. 10 in exploring validities of various assumptions used in the model.

Resin losses in the vertical and horizontal directions can be calculated as well with this model. Fig. 12 shows the volumetric resin loss,  $Q_z$ , in the vertical direction according to Eq. (4) for different values of  $C_z Z_0$ . It is obvious that the larger the pressure drop  $C_z Z_0$  is, the higher the resin loss in the z-direction becomes. The ratio of  $Q_z$  to the total resin loss can be calculated by combining Eqs. (4) and (13).

$$\frac{Q_z}{Q_T} = - C_z K \int_0^t \frac{1}{\eta(t)} dt / \int_0^t \dot{h} dt, \quad (20)$$

where the second integral can be evaluated from Fig. 7.

#### IV. CONCLUSIONS

A theory which describes the resin consolidation process during prepreg lamination has been formulated. It is based on the assumption that the system is composed of two types of flow: a horizontal squeezing flow between two nonporous parallel plates, and a vertical poiseuille type pressure flow through porous media. Flows in all directions originate from the squeezing action between two approaching fiber/fabric layers which are subjected to an external load  $F$ . A parametric study reveals that model predictions are in reasonable qualitative agreement with physical observations. Quantities such as resin loss during lamination, velocity and pressure profiles associated with resin flows, laminate consolidation speed and prepreg processibility, etc., can all be calculated. The interrelationships between these quantities have been illustrated. Potential uses of the model in quality control of incoming prepreg materials have been discussed as well. Confirmations of the prepreg characterization methods, as suggested in the theory by experimental measurements, have been planned. The parallel-plate plastometer will be an appropriate device to verify the model.

## REFERENCES

1. Hou, T. H.: "Chemoviscosity Modelling for Thermosetting Resins-I," NASA CR-172443, 1984.
2. Bartlett, C. J.: "Use of the Parallel Plate Plastometer to Characterize Glass-Reinforced Resins: I. Flow Model," *Elastomers & Plastics*, 10, 369, 1978.
3. Bloechle, D. P.: "Use of the Parallel Plate Plastometer to Characterize Glass-Reinforced Resins: II. Experimental Results for B-Stage Epoxy Materials," *Elastomers & Plastics*, 10, 377, 1978.
4. Bloechle, D. P.: *Circuit World*, 9, No. 1, 8, 1982.
5. Springer, G. S.: "A Model of the Curing Process of Epoxy Matrix Composite Materials," *Progress in Science and Engr. of Composites*, T. Hayashi, K. Kawata and S. Umekawa Eds., Japan Soc. Compo. Matl., 23, 1982.
6. Loos, A. C.; and Springer, G. S.: "Calculation of Cure Process Variables During Cure of Graphite-Epoxy Composites," *Composite Materials: Quality Assurance and Processing*, E. C. Browning Ed., ASTM STP 787, 110, 1983.
7. Springer, G. S.: "Resin Flow During the Cure of Fiber Reinforced Composites," *J. Compo. Matl.*, 16, 400, 1982.
8. Loos, A. C.; and Springer, G. S.: "Curing of Epoxy Matrix Composites," *J. Compo. Matl.*, 17, 135, 1983.
9. Lindt, J. T.: "Engineering Principles of the Formation of Epoxy Resin Composites," *SAMPE Quarterly*, 14, October 1982.
10. Muskat, M.: "Flow of Homogeneous Fluids Through Porous Media", McGraw-Hill, 1937.
11. Bird, R. B.; Armstrong, R. C.; and Hassager, O.: "Dynamics of Polymeric Liquids", John Wiley & Sons, 1977.



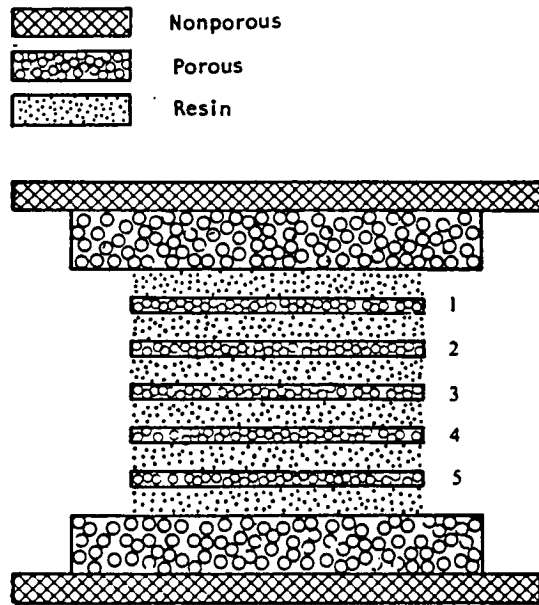


Figure 1. Schematic diagram of multilayer prepreg laminate

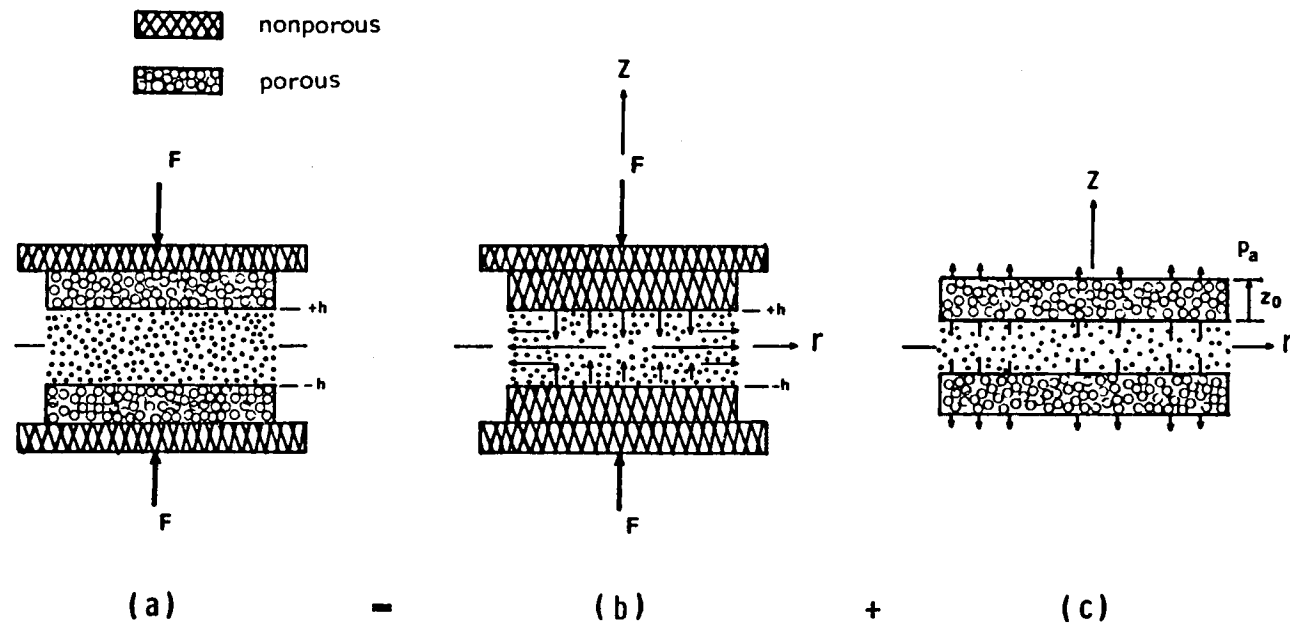


Figure 2. Resin flow - physical model

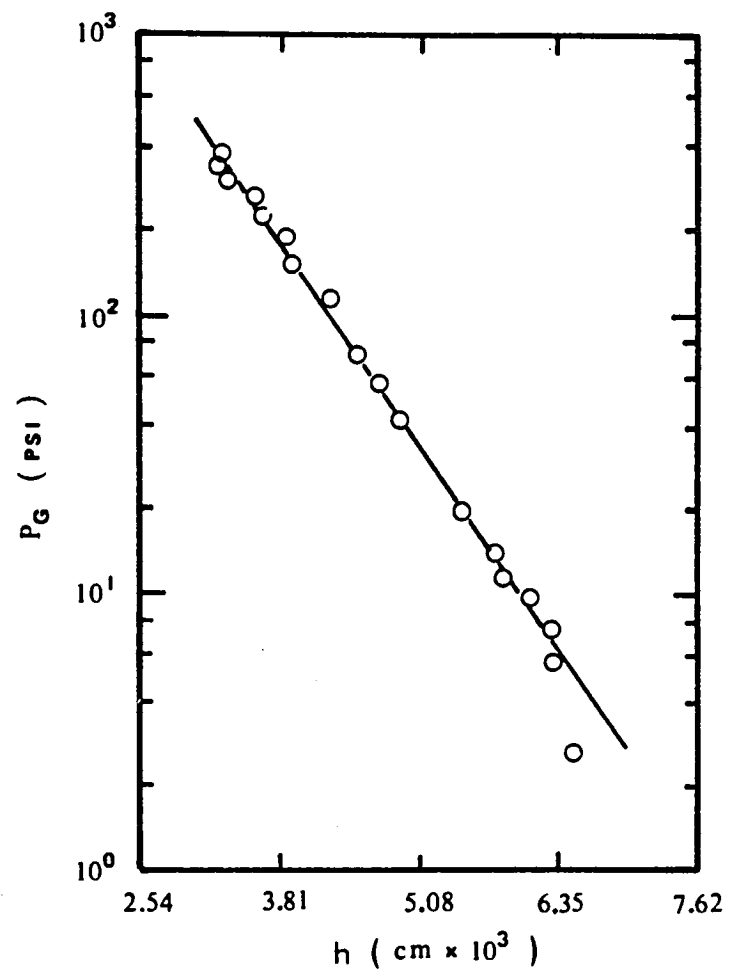


Figure 3. Compression data for 1080 glass fabric (Bartlett, Ref. 2)

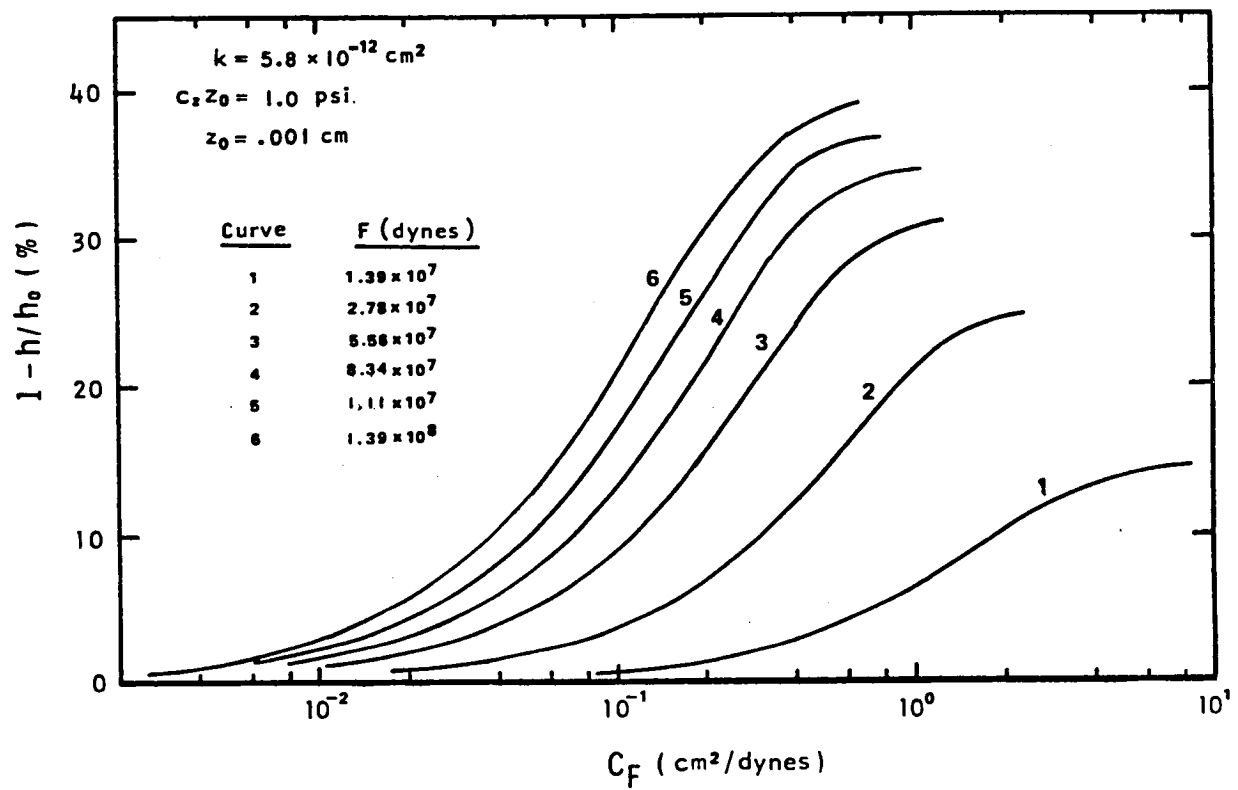


Figure 4. Changes of prepreg thickness vs. flow parameter at different values of applied load, F

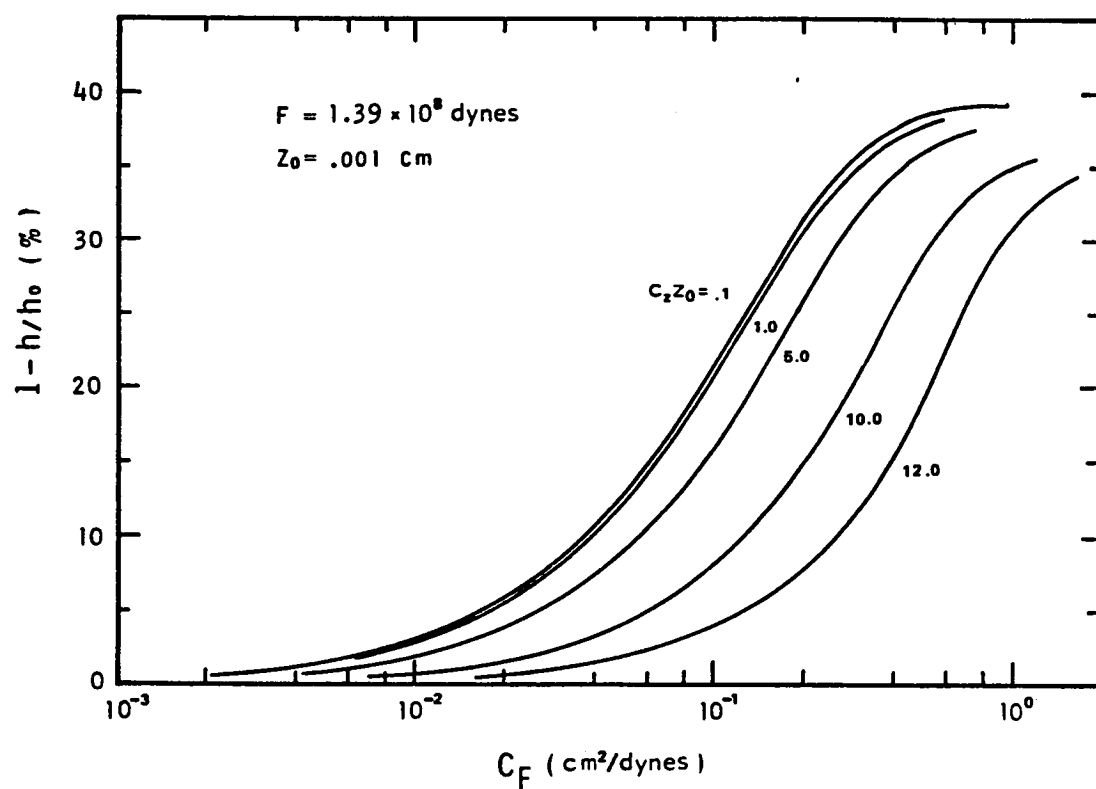


Figure 5. Changes of prepreg thickness vs. flow parameter at different values of  $C_z Z_0$

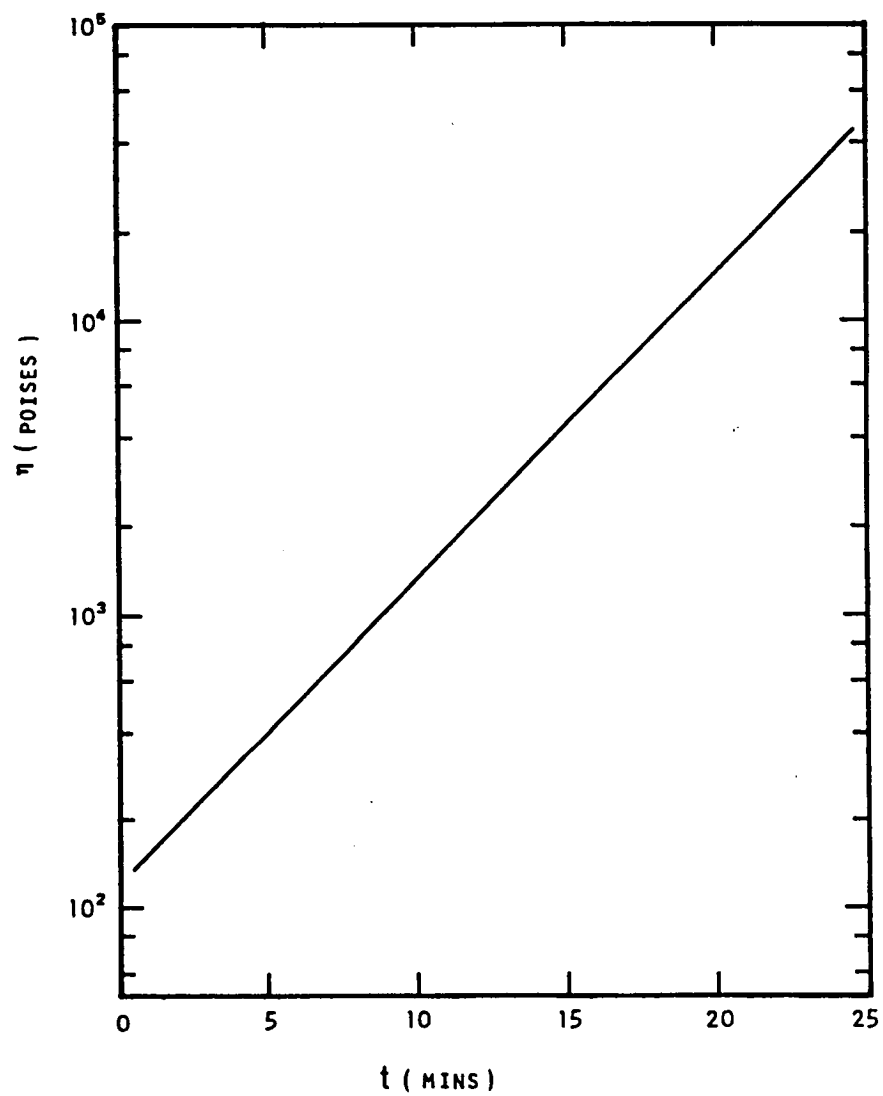


Figure 6. Chemoviscosity of a hypothetical B-stage epoxy resin at  $150^{\circ}\text{C}$  ( $423^{\circ}\text{K}$ )

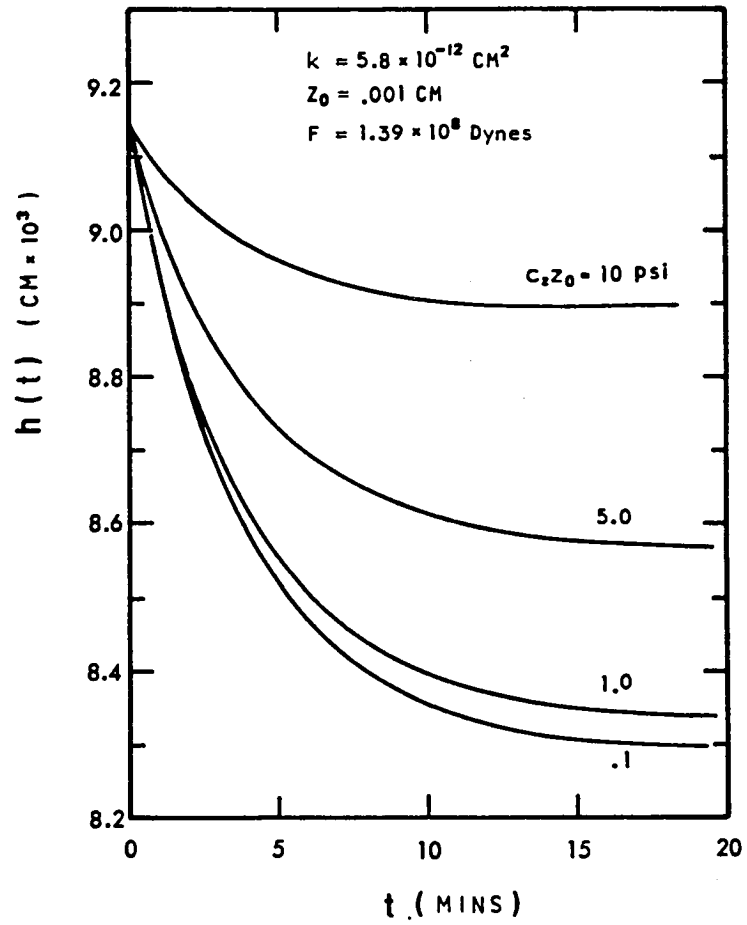


Figure 7. Variations of prepreg thickness as a function of time for different values of  $C_z Z_0$

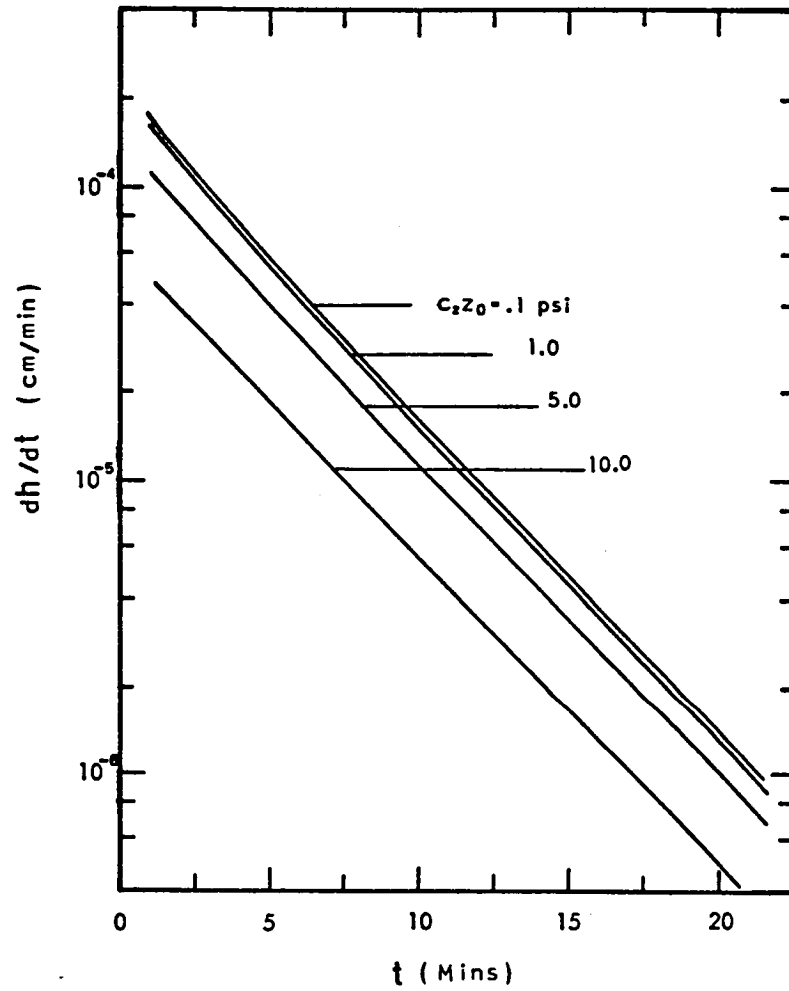


Figure 8. Rate of change of prepreg thickness as a function of time for different values of  $C_z Z_0$



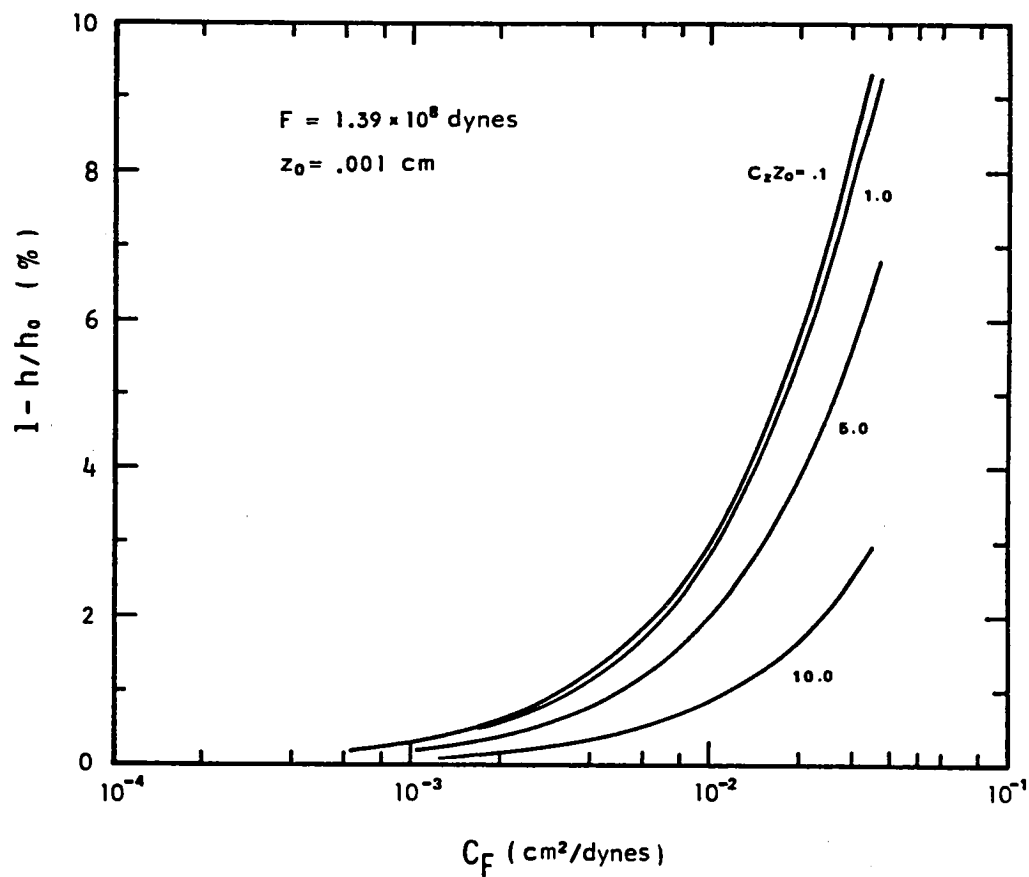


Figure 9. Changes of prepreg thickness vs. flow parameter at different values of  $C_z Z_0$

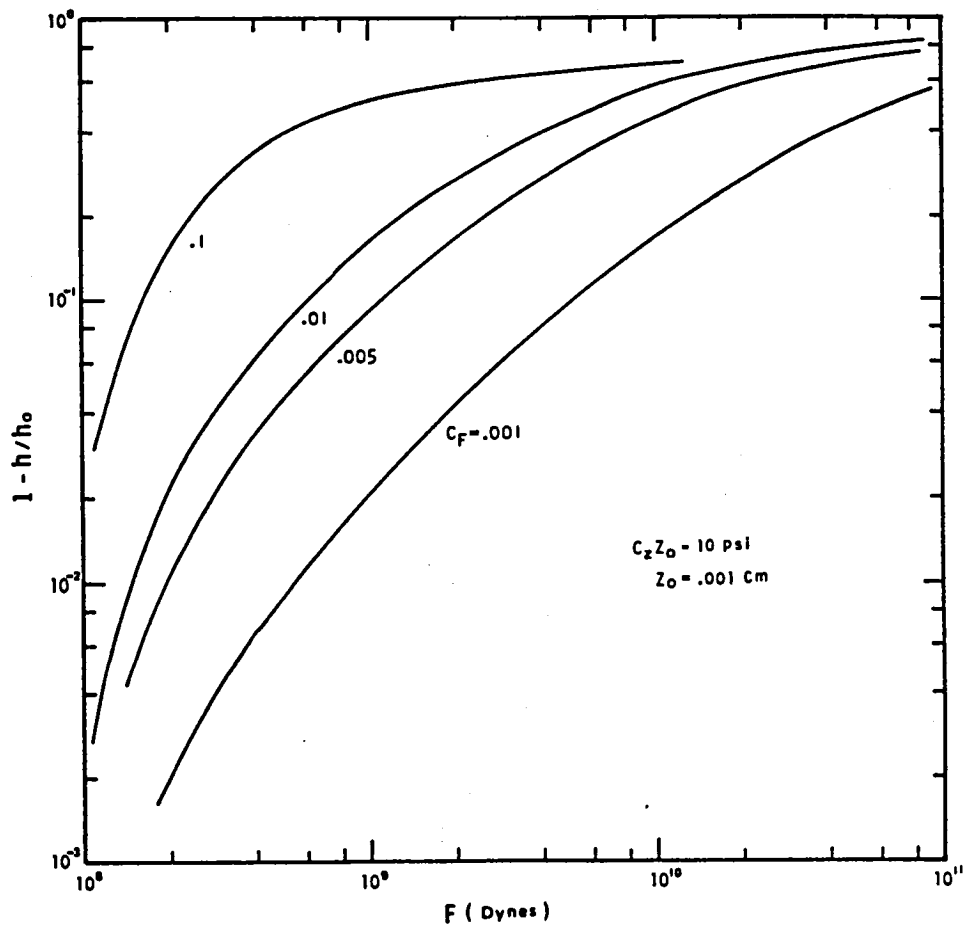


Figure 10. Changes of prepreg thickness vs. applied load at different values of flow parameter  $C_F$

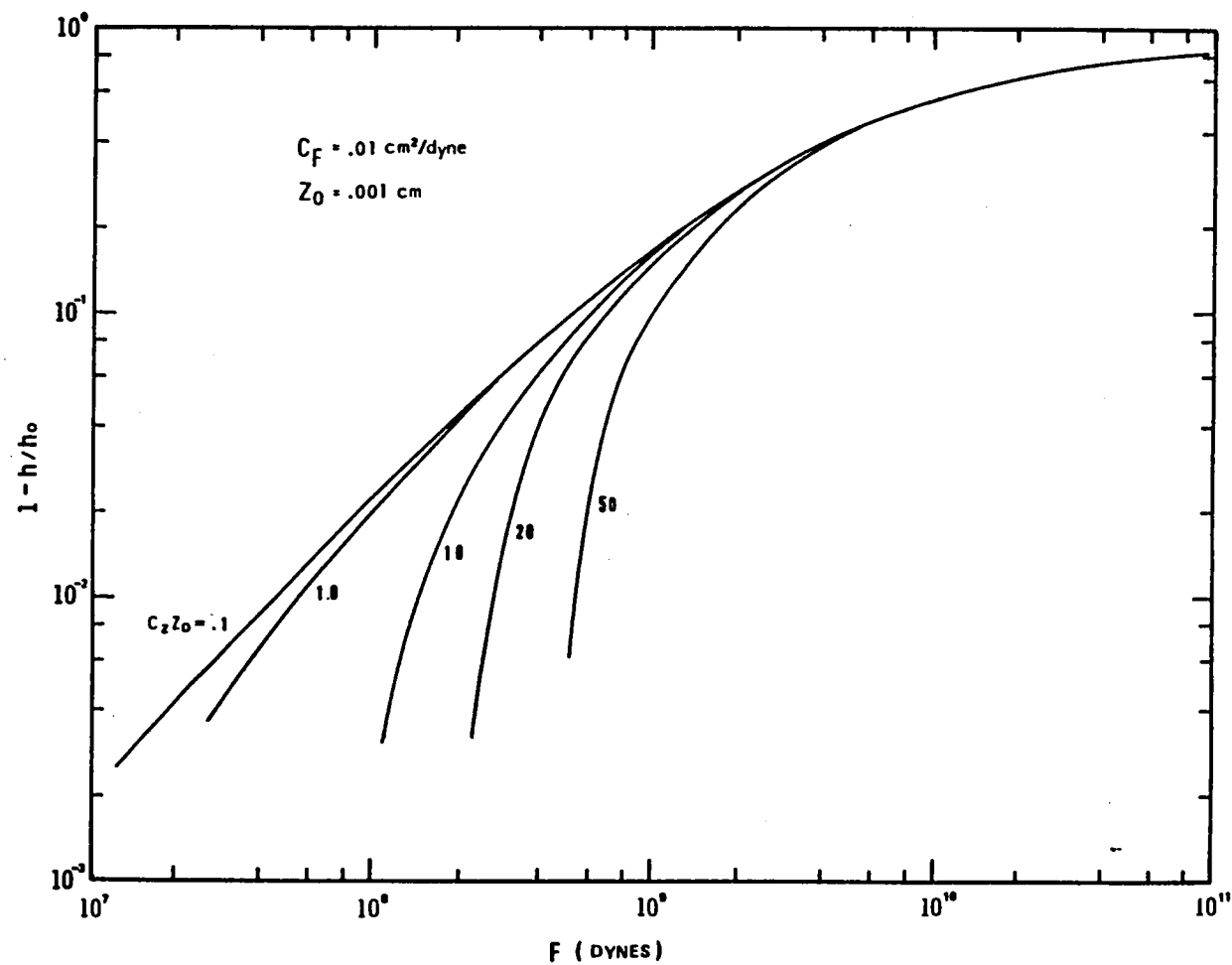


Figure 11. Changes of prepreg thickness vs. external load at different values of  $C_Z Z_0$

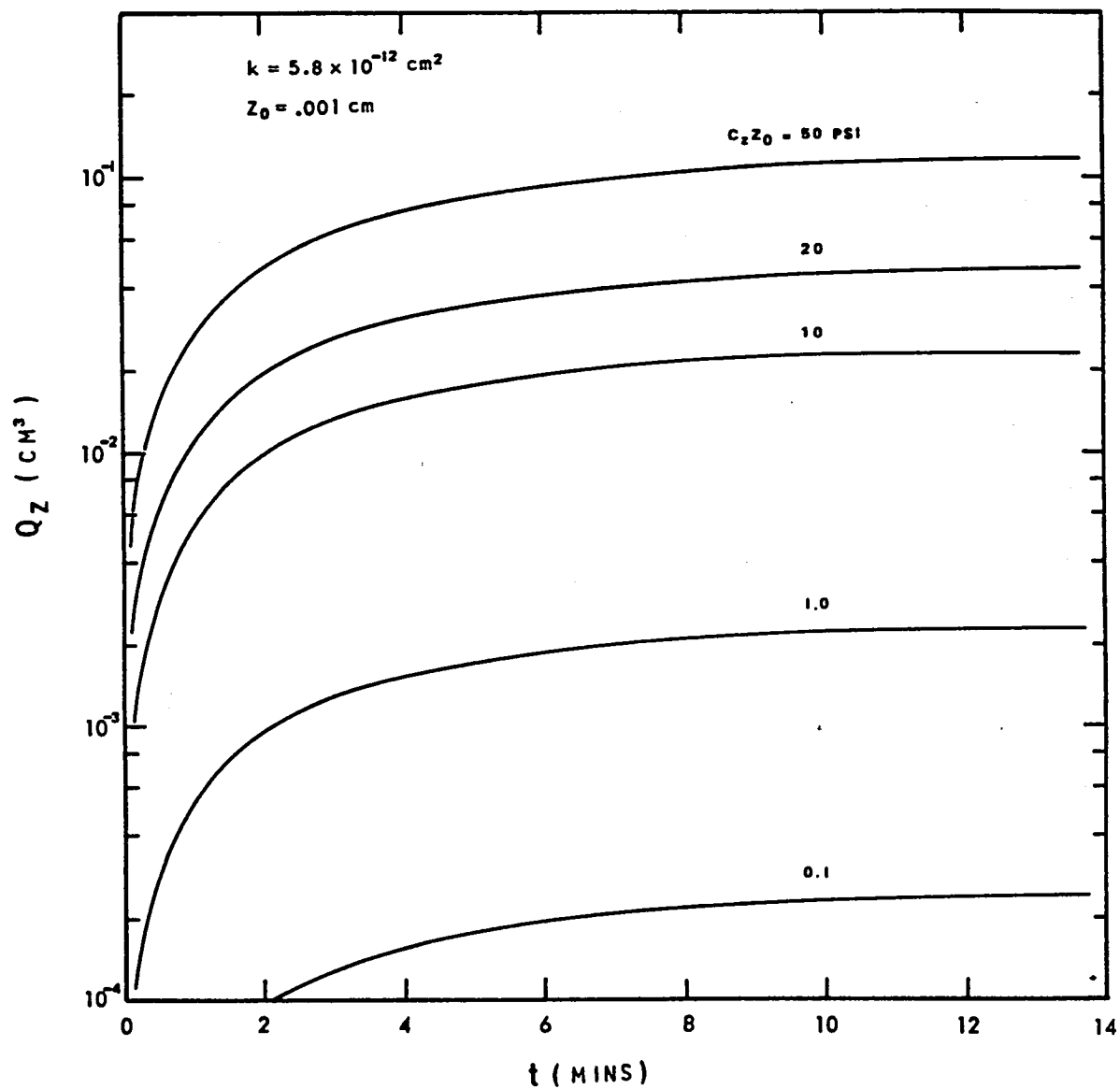


Figure 12. Volumetric resin flow in the vertical direction as a function of time at different values of  $C_z Z_0$



1. Report No. NASA CR-172442		2. Government Accession No.		3. Recipient's Catalog No.	
4. Title and Subtitle A Theoretical Study of Resin Flows for Thermosetting Materials During Prepreg Processing				5. Report Date July 1984	
				6. Performing Organization Code	
7. Author(s)  T. H. Hou				8. Performing Organization Report No.	
				10. Work Unit No.	
9. Performing Organization Name and Address Kentron International, Inc. 3221 North Armistead Avenue Hampton, VA 23666				11. Contract or Grant No.  NAS1-16000	
				13. Type of Report and Period Covered Contractor Report	
12. Sponsoring Agency Name and Address National Aeronautics and Space Administration Washington, DC 20546				14. Sponsoring Agency Code 505-33-33-01	
15. Supplementary Notes  Langley Technical Monitor: R. M. Baucom Final Report					
16. Abstract <p>A new flow model which describes the process of resin consolidation during prepreg lamination has been developed. A parametric study has also been carried out to explore the salient features of model predictions. It is assumed that resin flows in all directions are originated from squeezing action between two approaching adjacent fiber/fabric layers. In the horizontal direction, a squeezing flow between two nonporous parallel plates is analyzed, while in the vertical direction a poiseuille type pressure flow through porous media is assumed. Proper force and mass balances have been established and solved for the whole system which is composed of these two types of flow.</p> <p>A flow parameter, <math>C_F</math>, has been defined and shown to be a measure of processibility for the curing resin. For a given external load <math>F</math> the responses of resin flow during prepreg lamination, as measured by <math>C_F</math>, are categorized into three regions: the low <math>C_F</math> region where resin flows are inhibited by the high chemoviscosity during initial curing stages; the median <math>C_F</math> region where resin flows are properly controllable; and the high <math>C_F</math> region where resin flows are ceased due to fiber/fabric compression effects. Resin losses in both directions can be calculated as well.</p> <p>Potential uses of this model including quality control of incoming prepreg material are discussed. Experimental measurements needed to confirm the prepreg characterization methods suggested by the model have been planned for the future research. The parallel-plate plastometer will be an appropriate device to carry out the experiments.</p>					
17. Key Words (Suggested by Author(s))  Thermoset, Flow Model Squeezing Flow, Plastometer, Porous Materials			18. Distribution Statement  Unclassified - Unlimited  Subject Category 27		
19. Security Classif. (of this report) Unclassified		20. Security Classif. (of this page) Unclassified		21. No. of Pages 33	
				22. Price* A03	



